Journal of
Clinical Medicine

MDPI

Article

Is ovarian tissue transplantation safe in patients with central nervous system primitive neuroectodermal tumors?

Thu Yen Thi Nguyen [1,5], Alessandra Camboni [1,2,5], Rossella Masciangelo [1], Jacques Donnez[3] and Marie-Madeleine Dolmans [1,4] *

[1] Gynecology Research Unit, Institut de Recherche Expérimentale et Clinique, Université Catholique de Louvain, Av. Mounier 52, 1200 Brussels, Belgium; thu.nguyen@uclouvain.be (T.Y.T.N.); alessandra.camboni@gmail.com (A.C.); rossella.masciangelo@uclouvain.be (R.M.)
[2] Department of Anatomopathology, Cliniques Universitaires Saint-Luc, Av. Hippocrate 10, 1200 Brussels, Belgium
[3] Society for Research into Fertility, Av. Grandchamp 143, 1150 Brussels, Belgium; jacques.donnez@gmail.com (J.D.)
[4] Department of Gynecology, Cliniques Universitaires Saint-Luc, Av. Hippocrate 10, 1200 Brussels, Belgium
[5] These authors contributed equally to this work and share first authorship.

* Correspondence: marie-madeleine.dolmans@uclouvain.be; Tel.: +32-(0)2-764-5237; Fax: +32-(0)2-764-9507

Received: date; Accepted: date; Published: date

Abstract: The risk of reseeding malignancy harbored in cryopreserved and transplanted ovarian tissue has been a source of concern. This study aims to determine the potential relationship between frozen-thawed ovarian tissue transplantation and primary cancer recurrence. Three patients with cerebral primitive neuroectodermal tumors (PNET) were included in this study. One woman gave birth to three healthy babies following reimplantation of her cryopreserved ovarian tissue, but subsequently died due to cancer relapse 6 years after ovarian tissue transplantation. The second subject died from progressive cancer, while the third is still alive and awaiting reimplantation of her ovarian tissue in due course. Frozen ovarian cortex from all 3 patients was analyzed and xenotransplanted to immunodeficient mice for 5 months. Main outcomes were the presence of cancer cells in the thawed and xenografted ovarian tissue at histology, immunostaining (expression of neuron-specific enolase and glial fibrillary acidic protein (GFAP)), and reverse transcription droplet digital polymerase chain reaction (RT-ddPCR) (levels of enolase 2 and GFAP). In conclusion, no malignant cells were detected in ovarian tissue from patients with PNET, even in those who experienced recurrence of the disease, meaning that the risk of reseeding cancer cells with ovarian tissue transplantation in these patients can be considered low.

Keywords: Ovarian tissue cryopreservation; ovarian tissue transplantation; primitive neuroectodermal tumors; minimal disseminated disease; neuron-specific enolase; glial fibrillary acidic protein.

1. Introduction

These days, a cancer diagnosis is no longer a death sentence for most patients. Indeed, anticancer treatments have become increasingly effective, yielding significant improvements in patient survival rates. A more recent focus has become the quality of life of survivors because these treatment modalities, especially high-dose chemotherapy, pose a threat to a woman's reproductive organs,

leading to premature ovarian insufficiency and subsequent infertility [1,2]. For this reason, an appropriate approach to fertility preservation is required prior to therapy.

For prepubertal patients and women who need to start treatment immediately, ovarian tissue cryopreservation offers a unique option [1,3]. Frozen-thawed ovarian tissue can be transplanted back to the pelvic cavity once cancer therapy is complete and the patient shows no signs of relapse [3]. This procedure results in restoration of ovarian activity in up to 93% of cases, with ovarian function maintained for 4-5 years [4,5], and sometimes up to 7 years [6], depending on the follicle reserve before cryopreservation. By 2018, there had been more than 130 live births reported after autotransplantation of ovarian tissue worldwide [2], and that figure has probably exceeded 200 by now [7].

Safety issues surrounding reimplantation of ovarian tissue from cancer patients have been a cause of concern for many years [8,9]. A number of studies have investigated the risk of reintroducing malignant cells together with the frozen-thawed ovarian tissue, which could induce recurrence of the primary tumor. Malignant cells have been detected in case of leukemia and borderline ovarian tumors, but minimal disseminated disease (MDD) has not been documented in ovarian tissue from patients with bone and soft tissue sarcoma or low-grade breast cancer [10-13]. According to global transplantation data, no relapses have been recorded in any site associated with ovarian tissue reimplantation [14].

Thirty-one women with neurological malignancies have so far had their ovarian cortex stored in our ovarian tissue biobank, accounting for 5% of indications for ovarian tissue cryopreservation. The present study reports three cases of central nervous system (CNS) primitive neuroectodermal tumors (PNET) including one subject who relapsed 6 years after ovarian tissue transplantation that resulted in the birth of three children. The second subject unfortunately died. The third is alive and awaiting transplantation of her ovarian tissue in the future. However, her ovarian tissue was collected one month after insertion of a ventriculoperitoneal (VP) shunt, which may increase the risk of cancer cell contamination of the peritoneal cavity [15]. Our aim was to determine the potential relationship between ovarian tissue transplantation and primary cancer recurrence by detecting the presence of malignant cells in cryopreserved ovarian tissue.

2. Experimental Section

2.1 Patients

Three subjects with PNET involved in the study. The first patient had successful natural conceptions and gave birth to three children as a result of ovarian tissue reimplantation, but she died due to her primary cancer relapse 6 year after the transplantation. The second died in the progress of her cancer. The third is now alive and in free-disease period. Use of human tissue from the patients was approved by the Institutional Review Board of the Université Catholique de Louvain on 2 June 2014 (IRB reference 2012/23MAR/125, registration number B403201213872).

2.2 Thawing of frozen ovarian strips

The patients' ovarian cortex were stored in the biobank. Cryovials were thawed according to previously described protocol [12]. Thawed strips were assigned for testing MDD and xenografting.

2.3 Xenografting

Female severe combined immunodeficient (SCID) mice (Charles River Laboratories, France) aged 6 weeks were used for the present study. Animal welfare was respected following guidelines approved by the Committee on Animal Research of the Université Catholique de Louvain on 19 June 2014 (reference 2014/UCL/MD/007). Appropriate housing and breeding conditions were strictly

applied, as previously reported [16]. The surgical procedure has already been described [11]. The mice were raised in sterile conditions and received frequent health checks. After 5 months' grafting, euthanasia was performed by cervical dislocation and grafted ovarian tissues were collected and tested for MDD by histology, immunohistochemistry (IHC), reverse transcription-droplet digital polymerase chain reaction (RT-ddPCR) as described below.

2.4 Histological analysis

A small fragment of frozen-thawed ovarian tissue was fixed in 4% formaldehyde and embedded in paraffin wax. Samples were serially sectioned every 5 μm and placed on microscopy slides. Every fifth section was stained with hematoxylin and eosin (H&E) (Merck, Darmstadt, Germany) for histological analysis to determine the presence of metastatic cells in ovarian fragments, as well as follicle viability before and after grafting. H&E slides of primary tumors were used for comparative purposes to detect malignant cells in ovarian tissue.

2.5 Immunohistochemical analysis

Samples from the primary tumors were obtained from the anatomopathology department to serve as positive controls. Negative controls issued from ovarian tissue biopsies from patients with benign uterine pathologies. Expression of the neuronal marker neuron-specific enolase (NSE) and glial fibrillary acidic protein (GFAP) were investigated on patient's CNS tumor samples, cryopreserved and post-grafted ovarian tissue. Immunohistochemical staining of NSE and GFAP were automatically performed using Ventana's ultraView Universal DAB detection kit on the BenchMark ULTRA IHC/ISH system (Roche, Basel, Switzerland). Rabbit primary NSE antibody (catalog number A598, lot 106, Dako Corporation, CA, USA) and rabbit polyclonal GFAP antibody (catalog number CP040A, B, C, lot 121806, Biocare Medical, CA, USA) were used. Tissue sections were subsequently incubated with ultraView horseradish peroxidase-conjugated multimer antibody reagent (Igs, Ventana Medical Systems, AZ, USA) and counterstained with hematoxylin.

2.6 Sample storage, RNA extraction and reverse transcription

Ovarian strips destined for molecular analysis were cut into small pieces, immediately submerged in 700 μL RNAlater RNA stabilization reagent (Qiagen, Ambion, Texas, USA), and stored at -20°C until use. RNA extraction from ovarian tissue was performed using the RNeasy Plus mini kit (catalog number 74104, Qiagen, Germany) following the manufacturer's instructions. The patients' CNS tumor samples embedded in paraffin block were processed using RNeasy FFPE Kit (catalog number 73504, Qiagen, Germany) following the manufacturer's protocol.

Extracted RNA was qualified with the NanoDrop 2000 spectrophotometer (Thermo Fisher Scientific, ND-2000, Wilmington, USA) and purity was checked by assessing $A_{260/280}$ ratios over 1.90, followed by immediate storage at -80°C. Complementary DNA (cDNA) synthesis was carried out using the Advantage RT-for-PCR kit (Takara, catalog number 639505, CA, USA) and 0.5 μg total RNA, according to the manufacturer's protocol. The mixture was then placed in the thermal cycler (Applied Biosystems, serial number 096S9030939, CA, USA) for 1 hour at 42°C, 5 minutes at 94°C, and 3 minutes at 4°C. All cDNA was kept frozen at -20°C.

2.7 Droplet digital PCR

The patients' cerebral PNET samples were used as positive controls to detect enolase 2 (ENO2) fusion transcripts with human primer ENO2 Hs00157360_m1 (Thermo Fisher Scientific, CA, USA) and GFAP (Hs00909233_m1) while ovarian tissue biopsies from ten patients with benign gynecological diseases served as negative controls. Two housekeeping genes used in the study were

Abelson murine leukemia viral oncogene homolog 1 (ABL1, Hs01104728_m1), and beta 2 microglobulin (B2M, Hs00187842_m1). Sequences of primers and probes were detailed in Supplementary Table S1.

Droplet digital PCR (ddPCR) was performed on a QX200 system (Bio-Rad Laboratories Inc., Hercules, CA, USA). Each 20 µl reaction mixture consisted of ddPCR™ Supermix for probes (no dUTP) (Bio-Rad Laboratories) for ENO2 assays, 10 ng of cDNA, and Tris-EDTA buffer, following previously reported protocol [17]. Data were analyzed with QuantaSoft™ software (Bio-Rad Laboratories). Target concentrations in each sample were expressed as ENO2 or GFAP copies per microliter.

2.8 Defining the limit of blank and limit of detection

The limit of blank (LOB) and limit of detection (LOD) of ENO2 and GFAP in human ovarian tissue measured by ddPCR were defined[18]. The blank sample was the pool of RNA from 10 healthy women's normal ovarian tissue, measured by testing 60 replicates and calculated using the following formula: $LOB = mean_{blank} + 1.645\ (SD_{blank})$[19]. LOD was determined by measuring tenfold serial dilution between patients' CNS tumors and blank sample, in which, each stage of dilution consisted of 8 replicates and calculated following formula: $LOD = LOB + 1.645\ (SD_{\text{low concentration sample}})$[19]. LOD serves as a threshold to determine the quantification of a marker in an ovarian tissue from patients with PNET by ddPCR as 'detected' or 'not detected' malignant cells in this sample.

2.9 Next generation sequencing

As no molecular biology markers in RT-ddPCR were found for patient 1, next generation sequencing (NGS) was performed in the hope of finding a specific gene profile for that disease. The primary tumor sample from the patient 1 was tested for genetic mutations in the glioma panel (including ATRX, BRAF, CDKN2A, CDKN2B, CIC, DAXX, EGFR, FOXR2, FUBP1, H3F3A, HIST1H3B, IDH1, IDH2, KEL, KRAS, LZTR1, MET, MSH6, NF1, NOP53, PDGFRA, PIK3CA, PIK3R1, PTEN, QKI, RB1, TP53, TP73, TSC1 and TSC2) by using a NGS technique. The detailed methodology of NGS is not described here. The patient's ovarian tissue was then checked by NGS when positive mutations were found in the primary tumor.

2.10 Statistical analysis

Results of ddPCR were calculated statistically using Graphpad Prism, version 8.0 for desktop (GraphPad Software Inc., CA, USA). A p-value <0.05 was considered significant.

3. Results

3.1 Patient Information

Patient 1

The patient underwent ovarian tissue cryopreservation followed by transplantation some years later. In 2001, a 17-year-old patient was diagnosed with supratentorial PNET on the right orbitofontal lobe of the cerebrum, and underwent two operations for tumor removal. Prior to commencing adjuvant chemotherapy, she was offered a laparoscopy to collect ovarian tissue from both ovaries. No histological evidence of malignancy was found in the retrieved cortical and medullary tissue. Ovarian tissue cryopreservation was performed by slow-freezing, yielding 7 cryotubes containing 4 strips each. Thereafter, the patient underwent and completed chemotherapy with 6 VIDE (vincristine, ifosfamide, doxorubicin and etoposide) cycles according to the Euro-Ewing 99 protocol. In 2002,

however, extra-neural PNET metastasis to the right lung was diagnosed and radical resection was required. This was followed by intensive chemotherapy (2 cycles of VAI [vincristine, actinomycin D and ifosfamide] in association with busulfan-melphalan) and stem cell autotransplantation. Radiotherapy was indicated at the tumor site at a dose of 45 Gy for 25 sessions, plus a booster of 5 doses of 54 Gy. Regular follow-up data revealed complete disappearance of this CNS cancer.

After her treatment, the patient developed secondary ovarian failure, with amenorrhea and elevated serum follicle-stimulating hormone (FSH) levels. She was then (2003) prescribed hormone replacement therapy (HRT) and continued her routine gynecological and oncological follow-up. She got married in 2008 and subsequently came to our gynecology outpatient clinic with a desire to conceive. Examinations and investigations were carried out to explore both gynecological and oncological indications. Her hormone profile 3 months after stopping HRT showed FSH, luteinizing hormone (LH) and estradiol levels of 45.5 mIU/mL, 16.8 mIU/mL and <10 pmol/L respectively, which confirmed her menopausal status. The patency of both fallopian tubes was demonstrated by hysterosalpingography. Transvaginal ultrasound revealed a uterus of 40x27x17 mm in diameter and endometrial thickness of 1.4 mm with a regular echographic pattern. The right and left ovaries measured 17x7 mm and 13x6 mm respectively, and no antral follicles were seen. There were no suspicious masses in the abdomen. The patient was therefore prescribed oral contraceptives (containing 150 micrograms of desogestrel and 20 micrograms of ethinyl estradiol, one pill per day) for a period of 3 months prior to ovarian tissue transplantation to reduce the FSH level [3]. From a neuronal perspective, her follow-up profile included brain magnetic resonance imaging (MRI), which showed her to be disease-free. Laparoscopic surgery for transplantation of frozen-thawed ovarian tissue was performed by senior surgeons (JD and MMD) in November 2008, 6 years after the patient finished her cancer treatment. During surgery, no malignant masses were detected in the peritoneal cavity, while both ovaries were atrophic (Supplementary Figure S1). They were both decorticated and the anatomopathological results confirmed an absence of follicles. Ovarian cortical strips (1x10 mm in diameter) were then grafted to the right (7 fragments) and left (6 fragments) ovaries.

The patient's hormone profile after ovarian tissue reimplantation is shown in Figure 1. Three and a half months after surgery, a first estradiol peak was detected (49pg/mL), concomitant with a drop in FSH (13mIU/mL) and appearance of a follicle seen at ultrasonography. She resumed spontaneous menstrual bleeding.

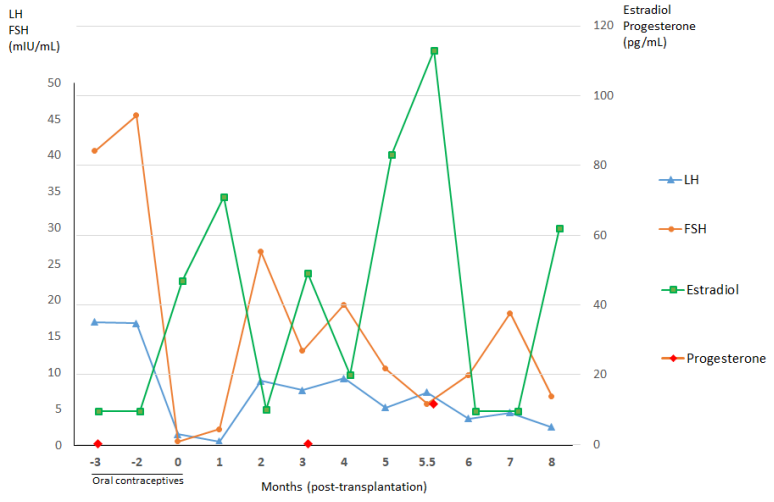

Figure 1. Hormone profiles before and after autografting of frozen-thawed ovarian tissue from patient 1. The transplantation procedure occurred at 0 months. Concentrations of estradiol rose 3 months after ovarian tissue transplantation with a concomitant drop in FSH, suggesting recovery of gonadal function. These hormone levels reached their peak 5.5 months postoperatively, when progesterone concentrations also increased. The patient subsequently conceived for the first time 9 months post-grafting.

FSH: Follicle-stimulating hormone; LH: luteinizing hormone.

Nine months after transplantation, she obtained her first pregnancy by natural conception and gave birth vaginally to a healthy baby boy in April 2010. She went on to have her second and third children in 2011 and 2012, after which she was prescribed oral contraceptives (containing multiphasic combinations of estradiol valerate [1-3mg] and dienogest [0-3mg], one pill per day). At the end of 2014, 12 years after her last radio-chemotherapy and 6 years after ovarian tissue transplantation, the patient relapsed with a nodule on the right frontal lobe of her cerebrum. This nodule was removed in its entirely in January 2015. The anatomopathological result confirmed recurrence of known PNET, without involvement of the cerebral parenchyma. The results of her CNS cancer extension profile, including cerebral MRI, thoracic MRI, positron emission tomography-computed tomography (PET-CT) imaging and histology of cerebrospinal fluid, were negative. The patient also completed adjuvant radio-chemotherapy involving 3 cycles of VAI and 2 cycles of vincristine and ifosfamide during radiotherapy at the tumor site (dose of 54 Gy delivered in 30 fractions of 1.8 Gy for 30 days). She developed refractory epilepsy in March 2015. In April 2016, she was admitted to hospital by the mobile emergency and resuscitation service, having suffered cardiopulmonary arrest at home after deterioration of her general condition and dyspnea for 3 days. She initially recovered from this asystole, with return of spontaneous circulation after 15 minutes of cardiopulmonary resuscitation, but experienced a second asystolic episode in the ambulance and was treated. On arrival at the hospital, she was diagnosed with hemodynamic instability and given vasopressor support (noradrenaline up to 50 gamma per minute). Paraclinical investigations found no hemorrhagic lesions upon brain CT scan imaging, nor pulmonary embolism on thoracic contrast CT. Conversely, cervical CT findings detected a thick mass next to the thyroid gland, restricting the trachea. MRI also identified tumor compression of the cervical cord (C2-D1) with leptomeningeal carcinomatosis, although previous MRI performed just 4 months before had shown no anomalies. This compression was thought to be the cause of neurogenic spinal shock and the initial cardiac arrest, requiring prolonged vasopressor support and mechanical ventilation, and gradually causing severe hypoxemia. She also suffered methicillin-sensitive Staphylococcus aureus (MSSA) bacteremia and responded to oxacillin treatment. However, after two weeks of treatment, the patient died from medullary compression caused by disseminated PNET. No autopsy was performed at the time as the family refused.

Patient 2

A 3-year-old patient was diagnosed with a PNET in her left frontal-parietal lobe in contact with the meninges in December 2012. She underwent subtotal resection surgery, but developed multiple meningeal nodular lesions in January 2013. Prior to chemotherapy, her ovarian cortex was collected by laparoscopy and cryopreserved by slow freezing protocol for fertility preservation. The patient was subjected to seven cycles of chemotherapy with a protocol for high-grade PNET and autologous stem cell transplantation before complete resection of the tumors in August 2013. She also underwent 17 sessions of radiotherapy in the following month. In October 2013, the subject was admitted to hospital with increased intracranial pressure. MRI revealed new multiple nodules disseminated in supra- and infratentorial regions and enlarged ventricles. An emergency VP shunt was inserted, but the patient died from cardiopulmonary arrest caused by neurological alterations after three weeks of treatment.

Patient 3

The patient was diagnosed with a grade IV PNET in the pineal region at the age of nine and underwent complete resection in August 2008 and insertion of a VP shunt one week later. One month later, laparoscopy was performed for ovarian tissue collection and cryopreservation prior to starting

radiotherapy targeting her tumor bed and cerebrospinal axis with 51 sessions in total. She is 20 years old now and free of disease.

3.2 Histology and immunohistochemistry

Morphologically normal primordial follicles in ovarian tissue from patient 1, patient 2 and patient 3 were identified at a mean density of 55.7 (SD 14.6), 45.2 (SD 12.1) and 56.2 (SD 7.4) follicles per mm^3 respectively.

All sections were negative for malignant cell presence at histology (Figure 2d, e and f). The patients' primary tumors were used as positive controls. These PNET cells, characterized by small round blue cells and rosette-like structures, are illustrated in Figure 2a, b and c.

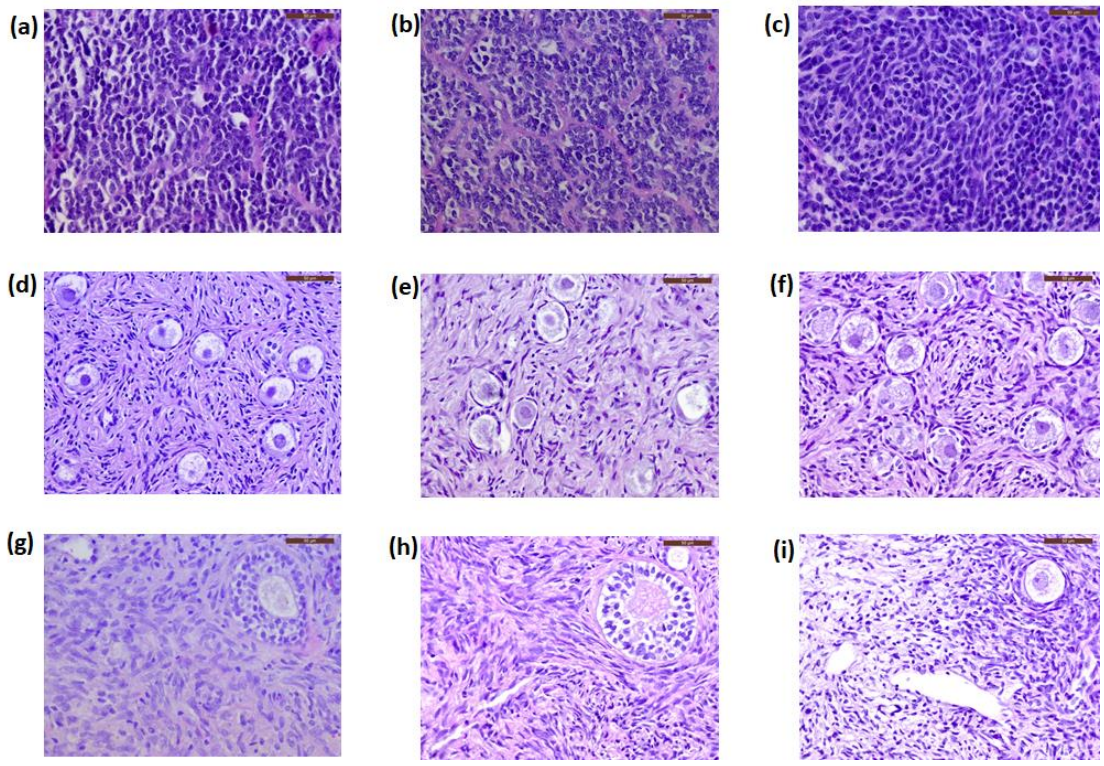

Figure 2. Histological sections of the primary tumors (PNET) and ovarian tissue from the patients. Primary tumors from patient 1 (a), patient 2 (b) and patient 3 (c) were characterized by small round blue cells and rosette-like structures. Frozen-thawed ovarian tissue (d), (e), (f) and ovarian tissue after long-term grafting (g), (h) and (i) showed no cancer cell contamination. Scale bars: 50 μm.

PNET: primitive neuroectodermal tumor.

By IHC, cryopreserved ovarian cortical tissues from all patients were negative for NSE expression (Figure 3d, e and f), while this marker was extensively expressed in their primary CNS tumors (Figure 3a, b and c) and patient 1's recurrent tumor. The primary tumor from patient 1 was negative for GFAP immunostaining, while those from patient 2 and patient 3 were positive for GFAP expression (Figure 4a and b). Cryopreserved ovarian tissue from patient 2 and patient 3 also showed no GFAP immunoexpression (Figure 4c and d).

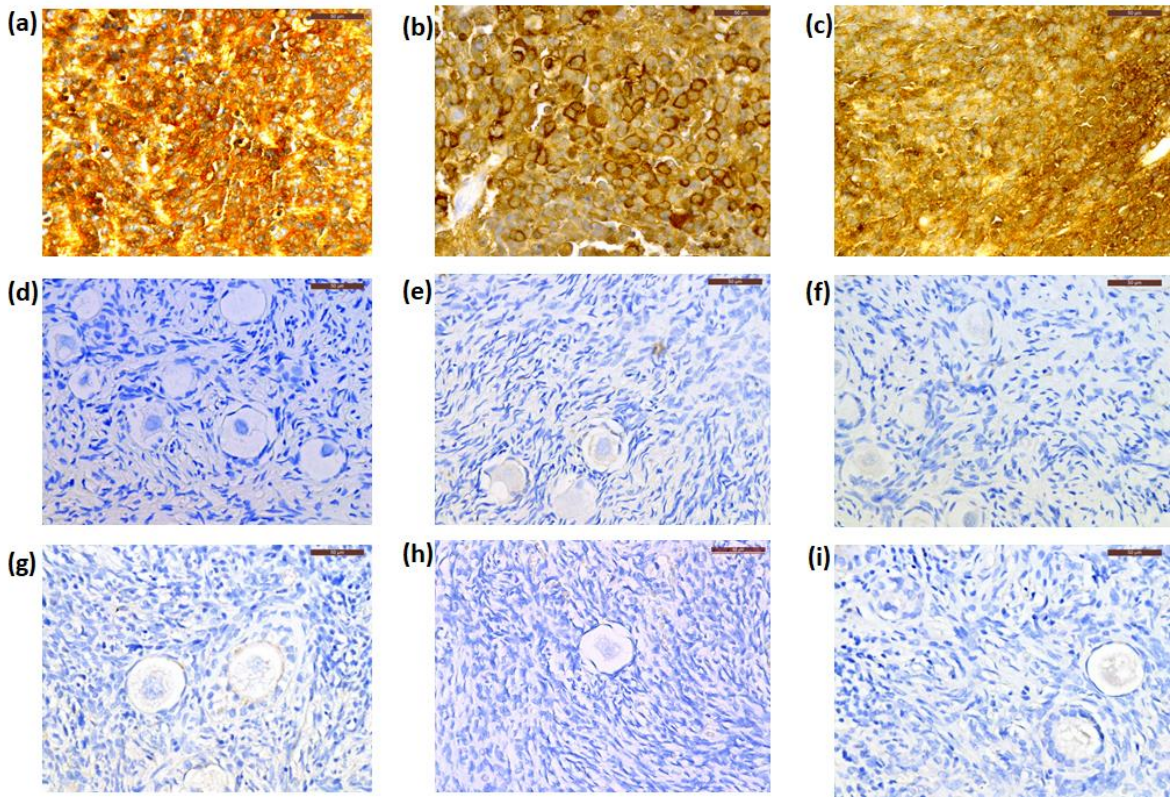

294

295 **Figure 3.** Representative photos of immunostaining for NSE in three patients. The primary tumor
296 (PNET) from patient 1 (a), patient 2 (b) and patient 3 (c) showed NSE positive expression, while
297 staining in frozen-thawed (d), (e) (f) and xenografted ovarian tissue (g), (h), (i) from patient 1, 2 and 3
298 were negative, respectively. Scale bars: 50 μm.

299 NSE: neuron-specific enolase; PNET: primitive neuroectodermal tumor.

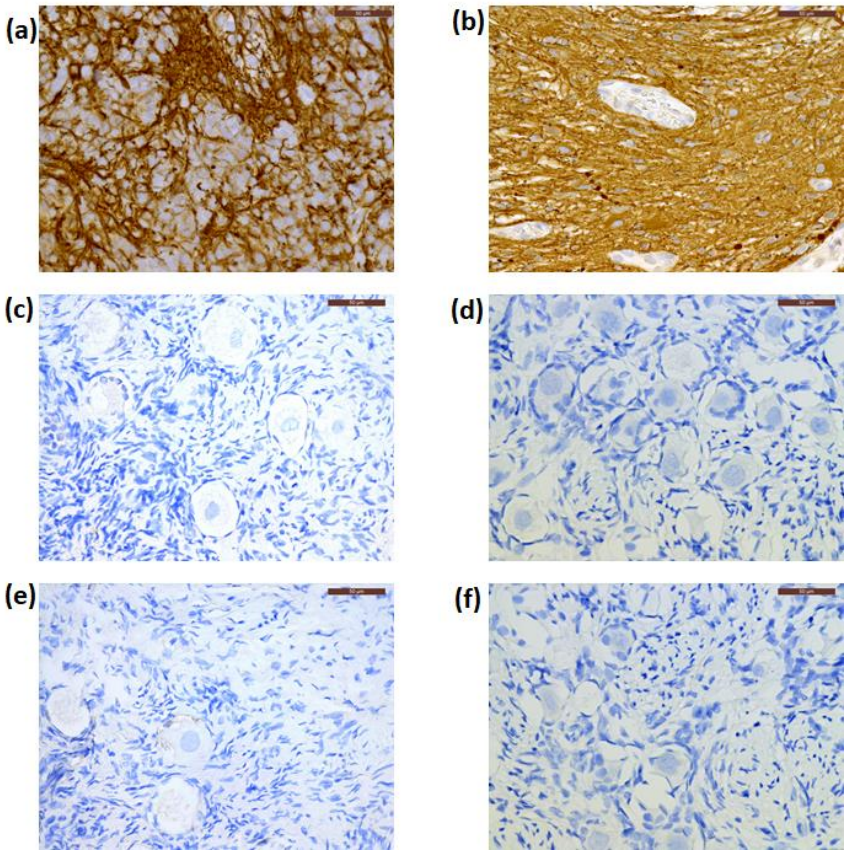

Figure 4. Immunostaining of GFAP in the primary tumor, cryopreserved and xenograted ovarian tissue from patient 2 (a, c, e) and patient 3 (b, d, f), respectively. These ovarian tissue showed negative expression of GFAP. Scale bars: 50 μm.

GFAP: glial fibrillary acidic protein.

3.3 Droplet digital PCR

The LOB of ENO2 in human ovarian tissue was defined by measuring the level of gene expression of 60 replicates of pooled normal ovarian samples from 10 healthy women, considered as negative controls, and was 28.5 copies/μl. As there was no significant difference between ENO2 concentrations in negative controls and the patients' primary tumors (positive control, Supplementary Figure S2), the ENO2 gene could not be used to determine the presence of PNET cell contamination in the patients' ovarian tissue. Indeed, positive signals for ENO2 were also obtained in normal ovarian cortex from 10 healthy women.

In contrast, the LOB of GFAP in human ovarian tissue was low, which was 0.1 copies/μl. The LOD values of GFAP for detecting the presence of PNET cells in ovarian tissue from patient 2 and 3 was 0.004 and more accurately resulted in 0.14 GFAP copies/μl (Figure 5). Levels GFAP gene expression were quantified absolutely by RT-ddPCR in cryopreserved ovarian tissue from patient 2 and patient 3, which was illustrated in Figure 6. No GFAP transcripts were detected in these samples, while those concentrations of positive controls were 183 (patient 2) and 196 (patient 3) copies/μl.

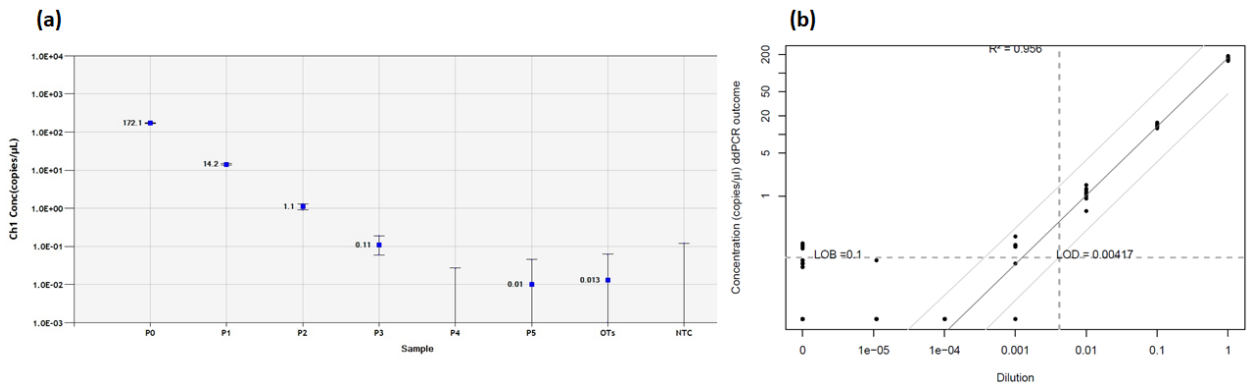

Figure 5. Determination of LOB and LOD of GFAP in human ovarian tissue from patients with PNET by RT-ddPCR. (a) Standard dilutions between primary tumors from patient 2 and patient 3 and pooled samples of 10 normal ovarian tissue. The x and y axes represent concentrations and dilutions respectively. (b) The LOB of GFAP in normal ovarian tissue was 0.1 copies/µl. LOD values of GFAP determined by serial dilutions between PNET samples (patient 2 and patient 3) and pooled sample of normal ovarian tissue were low, at 0.15 copies/µl with high linearity (R2>0.9).

LOB: limit of blank; LOD: limit of detection; GFAP: glial fibrillary acidic protein. OTs: pooled samples of normal ovarian tissue from 10 healthy women; NTC: no-template control. PNET: primitive neuroectodermal tumor.

Sample P1=100% PNET; P1=10% PNET + 90% OTs; P2=1% PNET + 99% OTs; P3=0.1% PNET + 99.9% OTs; P4=0.01% PNET + 99.99% OTs and P5=0.001% PNET + 99.999% OTs.

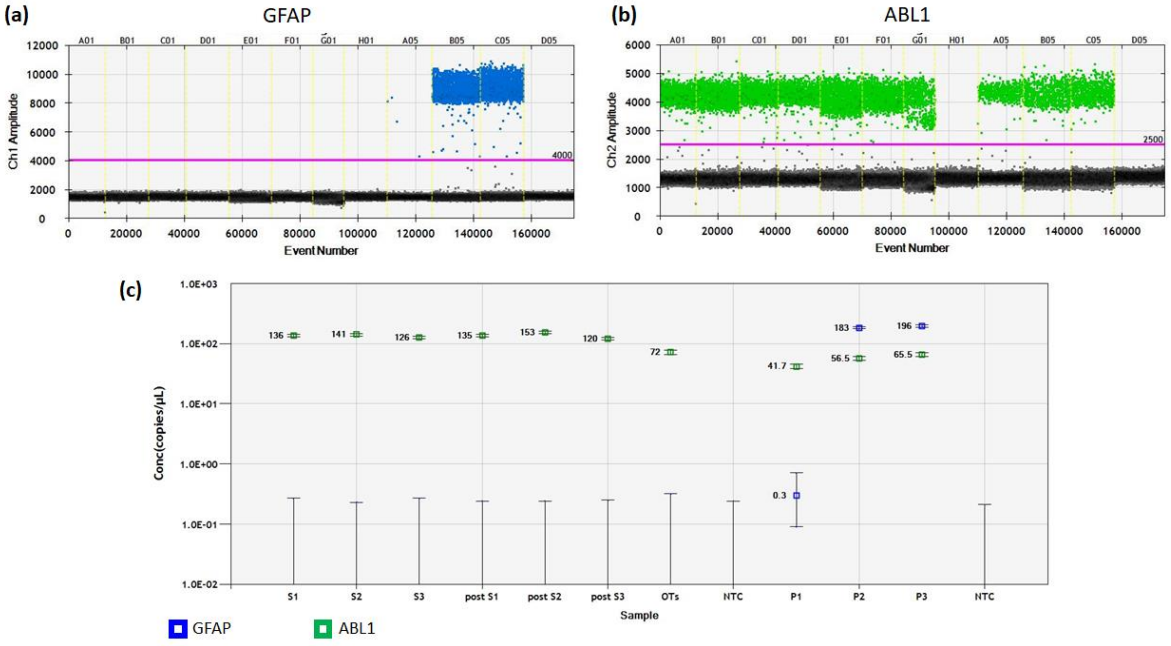

Figure 6. Detection of GFAP gene amplification in cryopreserved and xenografted ovarian tissue from three patients. **(a)** FAM fluorescent signals of GFAP transcripts in each droplet were plotted against the cumulative droplet count. The blue dots illustrate individual droplets containing at least one transcript copy. The black and grey dots represent negative droplets (background). No positive droplets were found in any no-template control wells (H01 and D05). **(b)** Plotting of VIC fluorescent dye for ABL1 in each well is shown. Patient samples, positive controls (PNET) and negative controls (normal ovarian tissue) contained green droplets, while no-template controls (well H01 and D05) showed no green signals. **(c)** Concentrations of samples were calculated with blue squares representing to GFAP transcripts and green squares ABL1 amplifications. No cancer cells were detected in all ovarian tissue samples.

GFAP: glial fibrillary acidic protein; PNET: primitive neuroectodermal tumor.

S1-3: cryopreserved samples from patient 1-3; Post s1-3: xenografted sample from patient 1-3; P1-3: primary tumor from patient 1-3 (positive control); OTs: pooled samples of normal ovarian tissue from 10 healthy woman (negative control); NTC: no-template control.

3.4 Next-generation sequencing

The purpose of NGS is to identify any mutations specific to the primary cancer from patient 1. If available, these mutations may be subsequently used as markers to detect the possibility of cancer cell spread to ovarian tissue. However, no mutations of genes of interest in the glioma panel were detected by NGS in the patient 1's primary tumor, so NGS analysis was not conducted on her ovarian samples.

3.5 Xenotransplantation

After 5 months of xenografting and frequent follow-up, there was no sign of disease in all the SCID mice used for this study. No suspicious masses were encountered in transplanted sites upon macroscopic evaluation. All the grafted tissue fragments had decreased in size. Human ovarian fragments from PNET patients were degrafted from the mice and investigated.

Ovarian follicles were observed at different developmental stages. Follicle density in ovarian tissue from patient 1, patient 2 and patient 3 after grafting was 21.4 (SD 9.9), 16.4 (SD 6.5) and 22.3 (SD 7.7) primordial follicles/mm^3 respectively. None of serial sections of the patients' ovarian tissue showed any evidence of cancer cells from histological analysis (Figure 2g, h and i). Similarly, none of the samples expressed NSE immunostaining (Figure 3g, h and i).

In xenografted ovarian tissue from patient 2 and patient 3, GFAP expression was also negative in IHC analysis (Figure 4e and f). In addition, these samples revealed no GFAP gene amplification detected by ddPCR (Figure 6). The absence of GFAP positive droplets in all no-template controls and the stable appearance of ABL1 housekeeping gene transcripts in this duplex ddPCR run highlighted the reliability of the test. Patients' information was detailed in table 1.

Table 1. Details of patients CNS PNET who underwent ovarian tissue cryopreservation

Patient n°	Age* (y)	Extraneural metastasis	Relapse	Alive or deceased	Cancer cells in histology	Immunohistochemistry			Concentration of GFAP transcripts by RT-ddPCR (copies/µl)	
						Patient CNS tumors	Cryopreserved OT	Xenografted OT	Cryopreserved OT	Xenografted OT
1	17	Yes, lungs	Yes	Deceased	No	**GFAP (-),** NSE (+)	NSE negative	NSE negative	0	0
2	4	No	No	Deceased	No	GFAP (+), NSE (+)	Both negative	Both negative	0	0
3	9	No	No	Alive	No	GFAP (+), NSE (+)	Both negative	Both negative	0	0

(*): age at ovarian tissue collection; CNS: central nervous system; GFAP: glial fibrillary acidic protein; NSE: neuron-specific enolase; OT: ovarian tissue; PNET: primitive neuroectodermal tumor; RT-ddPCR: reverse transcription droplet digital polymerase chain reaction.

In summary, no malignancy reseeding was detected in the frozen-thawed ovarian tissue of our subjects by histology or IHC before or after long-term xenotransplantation. Analysis by RT-ddPCR

identified no GFAP transcripts in cryopreserved and xenotransplanted ovarian tissue from patient 2 and patient 3.

4. Discussion

Among subjects involved in this study, patient 1 received the reimplantation of her ovarian tissue after seven years of cryopreservation. Following transplantation, her spontaneous menstruation resumed after 4 months, which is consistent with the literature. Indeed, the recovery of ovarian functions after grafting generally takes 4 to 5 months and is achieved in more than 95% of cases [1-3,5]. Patient 1 gave birth to three healthy babies achieved by natural conception between 2009 and 2012, making her one out of just three patients to obtain three successive pregnancies and live births worldwide following one ovarian tissue transplantation attempt [20,21]. Due to recurrence of her original cancer, she died. Questions were raised as to whether this recurrence was the inevitable evolution of the primary cancer or linked to the reimplantation of ovarian tissue. Thorough investigations and evaluations were therefore carried out to exclude the presence of malignant cells in the frozen-thawed ovarian tissue of this patient with CNS-PNET.

CNS-PNETs are rare, highly aggressive neoplasms, contributing to only 2-3% of all childhood brain tumors [22]. Based on the 2007 World Health Organization (WHO) classification, PNETs are a group of embryonal tumors consisting of poorly differentiated or undifferentiated neuroepithelial cells, which can proliferate into neuronal cells, astrocytes, ependymal cells, melanoma cells and myocytes [23]. This makes them difficult to diagnose by routine histopathology [24]. In the most recent WHO classification of CNS tumors (2016), the term primitive neuroectodermal tumor or PNET was actually removed from the diagnostic glossary [25]. However, the cases reported here occurred prior to 2016 and the pathological diagnoses were confirmed on the basis of previous criteria, which is why the term PNET is still used here to describe this disease.

Despite improvements in treatment modalities, the prognosis of supratentorial PNET has been historically poor. Recurrence of malignancy is observed in 37-56% of patients and is considered to be the main cause of patient mortality [26-30]. The interval to recurrence usually ranges from 3 to 94 months [28,29,31]. A study by Perreault et al in 2013 revealed that 50% of relapsed patients did not respond to treatments and often died 6 to 28 months after diagnostic confirmation of their recurrence [28].

It is known that a certain proportion of relapsing patients will eventually develop diffuse leptomeningeal dissemination, which may be related to genetic mutations [28,29]. Patient 1 in our study suffered a local relapse 12 years after her last chemotherapy session and 6 years after ovarian tissue reimplantation. She was diagnosed with intracranial recurrence on the frontal lobe and underwent multi-therapeutic management. However, 4 months after completion of treatments, the disease evolved and she developed leptomeningeal diffusion and medullary compression leading to death. Patient 2 deceased in the similar situation with the spread of meningeal nodules.

Extracranial metastases of CNS-PNET are infrequently reported in the literature. Most commonly mentioned sites of metastasis are regional lymph nodes, lungs and vertebral bones [32-34]. Our patient 1 also suffered pulmonary metastasis one year after complete resection of her primary tumor. Metastases regularly occur in patients undergoing cranial surgery, suggesting that local mechanical barriers may play a crucial role in disseminating cancer cells outside the CNS [33,35]. A likely explanation is that craniotomy may rupture vascular channels, resulting in the spread of malignant cells through blood and lymph vessels to extracranial sites. Peritoneal seeding of CNS cancers has been found, especially in patients who have VP shunt insertion [15]. It is because this shunt plays a role as an initial pathway for cancer cells appearing in cerebrospinal fluid to spread to the abdominal cavity. Patient 3 in our study, a prospective candidate for ovarian tissue transplantation in future, received VP shunt before ovarian tissue collection and cryopreservation. Testing for MDD in her ovarian tissue, thus, holds great importance. Our investigations showed that her cryopreserved and xenografted ovarian tissue were not contaminated by malignant cells, as confirmed by histology, IHC and ddPCR. To date, metastasis of CNS-PNET to the ovaries has not

been reported in the literature, but several cases of peripheral PNET originating in the ovaries have been published (Table 2). It should be borne in mind, however, that cancers in these cases primarily stemmed from the ovaries, without any tumors in the CNS itself, which differs from our current cases.

Table 2. Case reports on peripheral primitive neuroectodermal tumors of the ovary

Authors	Patient age (y)	FIGO stage	Treatment	Complications	Follow-up
Kawauchi et al (1998)[36]	29	II	TAH + BSO + omentectomy + PALA + chemotherapy	NA	11 months DOD
Chow et al (2004)[37]	13	IV	Debulking + chemotherapy 2nd debulking + chemotherapy + radiotherapy	NA	17 months DOD
Demirtas et al (2004)[38]	25	IC	LSO + omentectomy + PLA + chemotherapy 2nd look laparotomy	Pelvic abscess after 2nd look laparotomy	2 years 2 births NED
Kim et al (2004)[39]	18	IIIC	RSO + omentectomy + PLA + PALA + chemotherapy + radiotherapy	Bowel obstruction	10 months DOD
Ateser et al (2007)[40]	28	IV	TAH + LSO + omentectomy + chemotherapy + radiotherapy	Neutropenia	13 months DOD
Anfinan et al (2008)[41]	31	IIIC	TAH + BSO + omentectomy + chemotherapy	NA	15 months DOD
Ostwal et al (2012)[42]	28	NA	LSO + chemotherapy + radical excision upon recurrence	NA	18 months DOD
Huang et al (2013)[43]	28	IA	LSO + omentectomy + PLA + chemotherapy	NA	28 months NED

BSO: bilateral salpingo-oophorectomy; DOD: died of disease; FIGO: Fédération Internationale de Gynécologie et d'Obstétrique; LSO: left salpingo-oophorectomy; NA: not available; NED: no evidence of disease; PALA: para-aortic lymphadenectomy; PLA: pelvic lymphadenectomy; RSO: right salpingo-oophorectomy; TAH: total abdominal hysterectomy

Recurrence of the original cancer after transplanting ovarian tissue has been reported in several studies. A review of worldwide data on OTT in 2018 reported 9 out of 230 women with malignant disease experiencing a relapse after ovarian tissue transplantation, but none of them was thought to be related to the reimplantation procedure [14].

5. Conclusions

In the present study, it is important to emphasize that the patient 1's transplanted ovarian tissue was confirmed to be without any detectable malignancy by histological analysis at the time of ovarian tissue cryopreservation and transplantation. Her remaining frozen tissue showed no contamination by cancer cells in histological sections either after thawing or long-term xenotransplantation. This ovarian tissue was also negative for NSE expression, even though this marker was strongly expressed in the patient's primary tumor and repeated tumor. Furthermore, no malignancy was detected in cryopreserved ovarian tissue from other two patients by histology, IHC for NSE and GFAP, RT-ddPCR for detection of GFAP gene transcripts, or xenotransplantation to SCID mice. Indeed, we did not find any relationship between the primary cancer relapse and reimplantation of the patients' cryopreserved ovarian tissue.

To conclude, no malignancy was detected in any ovarian tissue samples from our patients with CNS-PNET, but relapse and disease progression are more likely to occur with CNS-PNET, as it is the nature of the disease. In this study, there was no evidence to associate the recurrence of primary cancer with reimplantation of ovarian tissue.

Supplementary Materials: The following are available online at www.mdpi.com/xxx/s1, Supplementary Table S1: Primer and probe sequences; Supplementary Figure S1: Representative photo of patient 1's right ovary observed at the time of laparoscopic ovarian tissue transplantation; Supplementary Figure S2: Comparison of ENO2 gene expression between blank samples and patients' primary tumors.

Author Contributions: Conceptualization: J.D. and M.M.D.; methodology and experimental work: T.Y.T.N., A.C. and R.M.; surgeries: J.D. and M.M.D.; formal analysis: T.Y.T.N. and A.C.; writing – original draft preparation: T.Y.T.N. and A.C.; writing – review and editing: J.D. and M.M.D; supervision: M.M.D. All authors revised and agreed to the published version of the manuscript.

Funding: This study was supported by grants from the Fonds National de la Recherche Scientifique de Belgique – Excellence of Science (FNRS–EOS), (grant number 30443682 awarded to Marie-Madeleine Dolmans and Thu YT Nguyen, FNRS grant number 5/4/150/5 to Marie-Madeleine Dolmans, FNRS-PDR Convention T.0077.14 to Marie-Madeleine Dolmans, Télévie grant 7.4590.16 to Rossella Masciangelo, and the Foundation Against Cancer grant 2018-042 awarded to Alessandra Camboni, as well as private donations (Family Ferrero and viscount de Spoelberch).

Acknowledgment: The authors thank Mira Hryniuk, BA, for reviewing the English language of the manuscript.

Conflicts of Interest: The authors declare no competing financial interests in relation to this work.

References

1. Donnez, J.; Dolmans, M. Fertility preservation in women. *Nature Reviews Endocrinology* **2013**, *9*, 735-749, doi:10.1038/nrendo.2013.205.
2. Donnez, J.; Dolmans, M. Fertility Preservation in Women. *The New England journal of medicine* **2017**, *377*, 1657-1665, doi:10.1056/NEJMra1614676.
3. Donnez, J.; Martinez-Madrid, B.; Jadoul, P.; Van Langendonckt, A.; Demylle, D.; Dolmans, M. Ovarian tissue cryopreservation and transplantation: a review. *Hum Reprod Update* **2006**, *12*, 519-535, doi:10.1093/humupd/dml032.
4. Donnez, J.; Squifflet, J.; Jadoul, P.; Demylle, D.; Cheron, A.; Van Langendonckt, A.; Dolmans, M. Pregnancy and live birth after autotransplantation of frozen-thawed ovarian tissue in a patient with metastatic disease undergoing chemotherapy and hematopoietic stem cell transplantation. *Fertility and Sterility* **2011**, *95*, 1787.e1781-1787.e1784,, doi:10.1016/j.fertnstert.2010.11.041.
5. Donnez, J.; Dolmans, M.; Pellicer, A.; Diaz-Garcia, C.; Sanchez Serrano, M.; Schmidt, K.; Ernst, E.; Luyckx, V.; Andersen, C.Y. Restoration of ovarian activity and pregnancy after transplantation of cryopreserved ovarian tissue: a review of 60 cases of reimplantation. *Fertility and sterility* **2013**, *99*, 1503-1513, doi:10.1016/j.fertnstert.2013.03.030.
6. Kim, S.S. Assessment of long term endocrine function after transplantation of frozen-thawed human ovarian tissue to the heterotopic site: 10 year longitudinal follow-up study. *J Assist Reprod Genet* **2012**, *29*, 489-493, doi:10.1007/s10815-012-9757-3.

7. Dolmans, M.M. Trials and tribulations of in vitro fertilization after ovarian tissue transplantation. *Fertil Steril* **2019**, *112*, 817-818, doi:10.1016/j.fertnstert.2019.07.1347.
8. Dolmans, M.M.; Luyckx, V.; Donnez, J.; Andersen, C.Y.; Greve, T. Risk of transferring malignant cells with transplanted frozen-thawed ovarian tissue. *Fertil Steril* **2013**, *99*, 1514-1522, doi:10.1016/j.fertnstert.2013.03.027.
9. Dolmans, M.M.; Masciangelo, R. Risk of transplanting malignant cells in cryopreserved ovarian tissue. *Minerva ginecologica* **2018**, *70*, 436-443, doi:10.23736/s0026-4784.18.04233-8.
10. Dolmans, M.M.; Iwahara, Y.; Donnez, J.; Soares, M.; Vaerman, J.L.; Amorim, C.A.; Poirel, H. Evaluation of minimal disseminated disease in cryopreserved ovarian tissue from bone and soft tissue sarcoma patients. *Human reproduction (Oxford, England)* **2016**, *31*, 2292-2302, doi:10.1093/humrep/dew193.
11. Dolmans, M.M.; Marinescu, C.; Saussoy, P.; Van Langendonckt, A.; Amorim, C.; Donnez, J. Reimplantation of cryopreserved ovarian tissue from patients with acute lymphoblastic leukemia is potentially unsafe. *Blood* **2010**, *116*, 2908-2914, doi:10.1182/blood-2010-01-265751.
12. Masciangelo, R.; Bosisio, C.; Donnez, J.; Amorim, C.A.; Dolmans, M.M. Safety of ovarian tissue transplantation in patients with borderline ovarian tumors. *Human reproduction (Oxford, England)* **2018**, *33*, 212-219, doi:10.1093/humrep/dex352.
13. Fabbri, R.; Vicenti, R.; Magnani, V.; Pasquinelli, G.; Macciocca, M.; Parazza, I.; Paradisi, R.; Battaglia, C.; Venturoli, S. Cryopreservation of ovarian tissue in breast cancer patients: 10 years of experience. *Future oncology (London, England)* **2012**, *8*, 1613-1619, doi:10.2217/fon.12.152.
14. Gellert, S.E.; Pors, S.E.; Kristensen, S.G.; Bay-Bjørn, A.M.; Ernst, E.; Yding Andersen, C. Transplantation of frozen-thawed ovarian tissue: an update on worldwide activity published in peer-reviewed papers and on the Danish cohort. *J Assist Reprod Genet* **2018**, *35*, 561-570, doi:10.1007/s10815-018-1144-2.
15. Xu, K.; Khine, K.T.; Ooi, Y.C.; Quinsey, C.S. A systematic review of shunt-related extraneural metastases of primary central nervous system tumors. *Clinical neurology and neurosurgery* **2018**, *174*, 239-243, doi:10.1016/j.clineuro.2018.09.038.
16. Nisolle, M.; Casanas-Roux, F.; Qu, J.; Motta, P.; Donnez, J. Histologic and ultrastructural evaluation of fresh and frozen-thawed human ovarian xenografts in nude mice. *Fertility and Sterility* **2000**, *74*, 122-129, doi:https://doi.org/10.1016/S0015-0282(00)00548-3.
17. Lombard C A; Fabre A; Ambroise J; Ravau J; André F; Jazouli N; Najimi M; Stéphenne X; Smets F; Vaerman J L, et al. Detection of Human Microchimerism following Allogeneic Cell Transplantation Using Droplet Digital PCR. *Stem Cells International* **2019**, *2019*, doi:10.1155/2019/8129797.
18. National Committee for Clinical Laboratory Standards. Protocols for determination of limits of detection and limits of quantitation; approved guideline. In *NCCLS Document EP17-A*, Wayne, PA USA, 2004; Vol. 24 No. 34 p80.
19. Armbruster, D.A.; Pry, T. Limit of blank, limit of detection and limit of quantitation. *Clin Biochem Rev* **2008**, *29 Suppl 1*, S49-S52.
20. Andersen, C.; Silber, S.; Bergholdt, S.; Jorgensen, J.; Ernst, E. Long-term duration of function of ovarian tissue transplants: case reports. *Reprod Biomed Online* **2012**, *25*, 128-132, doi:10.1016/j.rbmo.2012.03.014.
21. Meirow, D.; Ra'anani, H.; Shapira, M.; Brenghausen, M.; Derech Chaim, S.; Aviel-Ronen, S.; Amariglio, N.; Schiff, E.; Orvieto, R.; Dor, J. Transplantations of frozen-thawed ovarian tissue demonstrate high reproductive performance and the need to revise restrictive criteria. *Fertility and Sterility* **2016**, *106*, 467-474, doi:https://doi.org/10.1016/j.fertnstert.2016.04.031.

538 22. Smoll, N.R.; Drummond, K.J. The incidence of medulloblastomas and primitive neurectodermal
539 tumours in adults and children. *J Clin Neurosci* **2012**, *19*, 1541-1544, doi:10.1016/j.jocn.2012.04.009.
540 23. Louis, D.N.; Ohgaki, H.; Wiestler, O.D.; Cavenee, W.K.; Burger, P.C.; Jouvet, A.; Scheithauer, B.W.;
541 Kleihues, P. The 2007 WHO classification of tumours of the central nervous system. *Acta Neuropathol*
542 **2007**, *114*, 97-109, doi:10.1007/s00401-007-0243-4.
543 24. Picard, D.; Miller, S.; Hawkins, C.E.; Bouffet, E.; Rogers, H.A.; Chan, T.S.Y.; Kim, S.-K.; Ra, Y.-S.;
544 Fangusaro, J.; Korshunov, A., et al. Markers of survival and metastatic potential in childhood CNS
545 primitive neuro-ectodermal brain tumours: an integrative genomic analysis. *The Lancet Oncology* **2012**,
546 *13*, 838-848, doi:https://doi.org/10.1016/S1470-2045(12)70257-7.
547 25. Louis, D.N.; Perry, A.; Reifenberger, G.; von Deimling, A.; Figarella-Branger, D.; Cavenee, W.K.;
548 Ohgaki, H.; Wiestler, O.D.; Kleihues, P.; Ellison, D.W. The 2016 World Health Organization
549 Classification of Tumors of the Central Nervous System: a summary. *Acta Neuropathol* **2016**, *131*, 803-
550 820, doi:10.1007/s00401-016-1545-1.
551 26. Kim, D.G.; Lee, D.Y.; Paek, S.H.; Chi, J.G.; Choe, G.; Jung, H.-W. Supratentorial primitive
552 neuroectodermal tumors in adults. *J Neurooncol* **2002**, *60*, 43-52, doi:10.1023/a:1020207902659.
553 27. Pizer, B.L.; Weston, C.L.; Robinson, K.J.; Ellison, D.W.; Ironside, J.; Saran, F.; Lashford, L.S.; Tait, D.;
554 Lucraft, H.; Walker, D.A., et al. Analysis of patients with supratentorial primitive neuro-ectodermal
555 tumours entered into the SIOP/UKCCSG PNET 3 study. *European Journal of Cancer* **2006**, *42*, 1120-1128,
556 doi:https://doi.org/10.1016/j.ejca.2006.01.039.
557 28. Perreault, S.; Lober, R.M.; Carret, A.-S.; Zhang, G.; Hershon, L.; Décarie, J.-C.; Yeom, K.; Vogel, H.;
558 Fisher, P.G.; Partap, S. Relapse patterns in pediatric embryonal central nervous system tumors. *J*
559 *Neurooncol* **2013**, *115*, 209-215, doi:10.1007/s11060-013-1213-4.
560 29. Biswas, A.; Mallick, S.; Purkait, S.; Roy, S.; Sarkar, C.; Bakhshi, S.; Singh, M.; Julka, P.K.; Rath, G.K.
561 Treatment outcome and patterns of failure in patients of non-pineal supratentorial primitive
562 neuroectodermal tumor: review of literature and clinical experience form a regional cancer center in
563 north India. *Acta Neurochir (Wien)* **2015**, *157*, 1251-1266, doi:10.1007/s00701-015-2444-2.
564 30. Stensvold, E.; Krossnes, B.K.; Lundar, T.; Due-Tønnessen, B.J.; Frič, R.; Due-Tønnessen, P.; Bechensteen,
565 A.G.; Myklebust, T.Å.; Johannesen, T.B.; Brandal, P. Outcome for children treated for medulloblastoma
566 and supratentorial primitive neuroectodermal tumor (CNS-PNET) - a retrospective analysis spanning
567 40 years of treatment. *Acta Oncol* **2017**, *56*, 698-705, doi:10.1080/0284186X.2017.1301679.
568 31. Jakacki, R.I.; Burger, P.C.; Kocak, M.; Boyett, J.M.; Goldwein, J.; Mehta, M.; Packer, R.J.; Tarbell, N.J.;
569 Pollack, I.F. Outcome and prognostic factors for children with supratentorial primitive
570 neuroectodermal tumors treated with carboplatin during radiotherapy: a report from the Children's
571 Oncology Group. *Pediatr Blood Cancer* **2015**, *62*, 776-783, doi:10.1002/pbc.25405.
572 32. Matar, N.; Bahri, K.; Kallel, J.; Boubaker, A.; Jemel, H. Extraneural Supratentorial Primitive
573 Neuroectodermal Tumor Metastasis: An Adult Case Report. *IJNS* **2017**, *06*, 210-212, doi:10.1055/s-0036-
574 1584597.
575 33. Terheggen, F.; Troost, D.; Majoie, C.B.; Leenstra, S.; Richel, D.J. Local recurrence and distant metastasis
576 of supratentorial primitive neuro-ectodermal tumor in an adult patient successfully treated with
577 intensive induction chemotherapy and maintenance temozolomide. *J Neurooncol* **2007**, *82*, 113-116,
578 doi:10.1007/s11060-006-9249-3.

34. Varan, A.; Sarı, N.; Akalan, N.; Söylemezoğlu, F.; Akyüz, C.; Kutluk, T.; Büyükpamukçu, M. Extraneural metastasis in intracranial tumors in children: the experience of a single center. *J Neurooncol* **2006**, *79*, 187-190, doi:10.1007/s11060-006-9123-3.
35. Rickert, C.H. Extraneural metastases of paediatric brain tumours. *Acta Neuropathol* **2003**, *105*, 309-327, doi:10.1007/s00401-002-0666-x.
36. Kawauchi, S.; Fukuda, T.; Miyamoto, S.; Yoshioka, J.; Shirahama, S.; Saito, T.; Tsukamoto, N. Peripheral primitive neuroectodermal tumor of the ovary confirmed by CD99 immunostaining, karyotypic analysis, and RT-PCR for EWS/FLI-1 chimeric mRNA. *Am J Surg Pathol* **1998**, *22*, 1417-1422, doi:10.1097/00000478-199811000-00013.
37. Chow, S.; Lin, M.; Shen, J.; Wang, S.; Jong, Y.; Chien, C. Analysis of chromosome abnormalities by comparative genomic hybridization in malignant peripheral primitive neuroectodermal tumor of the ovary. *Gynecol Oncol* **2004**, *92*, 752-760, doi:10.1016/j.ygyno.2003.11.027.
38. Demirtas, E.; Guven, S.; Guven, E.S.G.; Baykal, C.; Ayhan, A. Two successful spontaneous pregnancies in a patient with a primary primitive neuroectodermal tumor of the ovary. *Fertility and sterility* **2004**, *81*, 679-681, doi:10.1016/j.fertnstert.2003.08.036.
39. Kim, K.J.; Jang, B.W.; Lee, S.K.; Kim, B.K.; Nam, S.L. A case of peripheral primitive neuroectodermal tumor of the ovary. *Int J Gynecol Cancer* **2004**, *14*, 370-372, doi:10.1111/j.1048-891X.2004.014224.x.
40. Ateser, G.; Yildiz, O.; Leblebici, C.; Mandel, N.M.; Unal, F.; Turna, H.; Arikan, I.; Colcaki, D. Metastatic primitive neuroectodermal tumor of the ovary in pregnancy. *Int J Gynecol Cancer* **2007**, *17*, 266-269, doi:10.1111/j.1525-1438.2006.00761.x.
41. Anfinan, N.M.; Sait, K.H.; Al-Maghrabi, J.A. Primitive neuroectodermal tumor of the ovary. *Saudi Med J* **2008**, *29*, 444-446.
42. Ostwal, V.; Rekhi, B.; Noronha, V.; Basak, R.; Desai, S.B.; Maheshwari, A.; Prabhash, K. Primitive neuroectodermal tumor of ovary in a young lady, confirmed with molecular and cytogenetic results--a rare case report with a diagnostic and therapeutic challenge. *Pathol Oncol Res* **2012**, *18*, 1101-1106, doi:10.1007/s12253-012-9503-2.
43. Huang, B.; Horng, H.; Lai, C.; Chang, W.; Su, W.; Yen, M.; Wang, P. Peripheral primitive neuroectodermal tumor of the ovary with torsion. *Gynecology and Minimally Invasive Therapy* **2013**, *2*, 65-69, doi:https://doi.org/10.1016/j.gmit.2013.02.001.